

# Discovery of Small Molecule Inhibitors of Protein–Protein Interactions Using Combined Ligand and Target Score Normalization

Fergal P. Casey,<sup>†</sup> Emilie Pihan,<sup>†</sup> and Denis C. Shields\*

UCD Complex and Adaptive Systems Laboratory, UCD Conway Institute, and School of Medicine and Medical Sciences, University College Dublin, Dublin 4, Ireland

Received August 7, 2009

Docking experiments of multiple compounds typically focus on a single protein. However, other targets provide information about relative binding efficiencies that is otherwise lacking. We developed a docking strategy that normalized results in both the ligand and target dimensions. This was applied to dock 287 approved small drugs with 35 peptide-binding proteins, including 15 true positives. The combined docking score was normalized by drug and protein and by incorporating information on contact similarity to the template protein–peptide contacts. The 20 top ranking hits included 6 true positives, and three matches with suggestive evidence in the literature: the cardiac glycoside digitoxin may inhibit WW domain interactions, the 14-3-3  $\zeta$  protein may bind negatively charged ligands, and the nuclear receptor coactivator site may bind nuclear receptor agonists. Additionally, the Bcl-2 antiapoptotic protein is predicted to bind pargyline, and the antiapoptotic p53 interacting protein MDM2 is suggested to bind clofazimine. These predictions represent starting points for the experimental development of PPI inhibitors based on an existing database of approved drugs and demonstrate that two-dimensional normalization improves docking efficiency.

## INTRODUCTION

Cellular signaling, both extracellularly and intracellularly, relies heavily upon the physical interactions among proteins. Targeting such interactions is emerging as a goal of pharmaceutical research. The interaction interfaces between proteins may provide a greater diversity of targets and may allow more specific regulation than simply inhibiting the major output of a protein, such as its catalytic activity. However, many such interaction interfaces are large and will require larger drugs to inhibit them. An example is the design of a large imidazole molecule for the inhibition of MDM2/p53 interaction.<sup>1</sup> Computational modeling of potential drug and compound interactions with protein targets will likely be even more challenging than that for traditional drug targets with small deep pockets.

Prediction of compounds that disrupt protein interactions with proteins will typically require a priori structural models of the protein interaction complex, often derived by X-ray crystallography. The goal is then to find a compound that replaces one or other surfaces of the proteins, thus preventing their interaction,<sup>2</sup> or alternatively a compound that combines with both proteins to stabilize their interaction.<sup>3</sup> Here, we focus on the former, concentrating on short peptide ligands of peptide-binding domains. In this context, we seek to identify small compounds that resemble the (relatively) short peptide ligands. The peptide binding domains may form a variety of conformations: some provide a deep pocket or groove into which a peptide inserts; in other cases the peptide forms a strand in the  $\beta$  sheet of the peptide binding domain.

Feasible computational approaches to address this problem include pharmacophore searching<sup>4–6</sup> and compound docking.

Previous approaches<sup>6</sup> searched approved drugs with defined pharmacophore queries defined from common peptide binding motifs drawn from the database of eukaryotic linear motifs<sup>7</sup> (ELM) in complex with interacting protein domains. Here, we investigated whether a more computationally intensive approach, molecular docking, might reveal drug–peptide similarities not uncovered in pharmacophore searching. In order to evaluate the utility of the technique, we included a set of protein–small molecule complexes which have been structurally characterized by X-ray crystallography or NMR, which act as a true positive set in our docking experiments.

In docking, we aim to determine if compounds can establish the same interactions as the native ligands. Docking dynamically places the ligand within the binding site and, unlike pharmacophore matching, is able to incorporate important steric constraints and to approximate desolvation effects. We implemented a combined ligand and target normalization procedure, which we showed to improve the ability to rank true positives more highly and then improved this score further by combining the docking energy score with a score based on the number of similar interactions formed between the compound and the native ligand. We present interesting findings for computational binding of approved drug compounds to peptide binding domains and discuss the potential practical applications of this information.

## METHODS

**Selection of True Positives.** Fourteen cocrystal structures and one NMR model were selected from the Protein Data Bank (PDB), with the requirements that they have in the complex a protein and a small molecule that mimics a natural peptide. In the set, we sample different classes of proteins:

\* Corresponding author phone: 00 353 1 7165344; e-mail: denis.shields@ucd.ie.

<sup>†</sup> These authors contributed equally to this work.

hydrolases, one aspartic proteinase, proteins involved in cell adhesion, cell cycle, apoptosis, or blood clotting, a ligase, one blood coagulation factor, and one hormone/growth factor carrier (Table S1, Supporting Information).

**Selection of Peptide Binding Domains.** Twenty cocrystal structures were selected from the PDB representing a subset of eukaryotic linear motif (ELM) peptide binding domains in complex with peptides. We chose a diverse set of domains and preferentially chose those complexed with smaller peptides, to ensure the binding pocket was of a smaller size (Table S2). We also chose those structures with fewer crystal contacts.<sup>8</sup>

**Selection of FDA Drugs.** We downloaded a flat SDF file (Structure Data Format: a common molecular format) with FDA-approved drugs from the DrugBank Web site.<sup>9</sup> We used Molecular Operating Environment<sup>10</sup> to generate up to 50 3D conformations with the stochastic search option, using the flat SDF file as input, and recovered the minimum energy conformation for each drug based on evaluation of the Merck Molecular Force Field MMFF94. This conformation was used as the starting conformation of the drug during the docking procedure. We initially selected FDA drugs that have already been shown to have common pharmacophore points with ELM proteins,<sup>6</sup> consisting of 161 compounds, but also included FDA drugs without ELM pharmacophore point matches. We filtered the pharmacophore matched list by keeping only drugs with rotatable bonds below 10, and by clustering with 70% similarity between molecular fingerprints, and retaining the compound with smallest rotatable bonds from each cluster. In the set of FDA-approved drugs that do not have ELM pharmacophore query matches, to reduce the data set size further, we reclustered with 40% similarity between fingerprints and retained the compound with the smallest rotatable bonds for each new cluster. In total, 287 FDA-approved small molecule drugs were selected for docking, which represents a diverse set of approximately 21% of all small molecule FDA-approved drugs (Table S3).

**Docking Trials.** Docking was performed with the open source software AutoDock version 4.<sup>11,12</sup> The grid parameter file specifies the 3D search space by setting 60 points in each dimension, the center coordinates of the native ligand as the center of the grid, and 0.375 Å spacing between each point. The docking parameters specified a genetic algorithm to use for energy minimization and parameters for initial placement of ligand (initial translation: tran0 random, initial rotation: quat0 random) as well as 50 separate docking runs to perform and 2 500 000 energy evaluations to use in each run. Apart from placement of the center of the grid map ('gridcenter') at the centroid of the native ligand obtained from crystal structure coordinates, and the number of runs, which were determined to strongly affect performance on an initial smaller redocking trial (data not shown), all parameters were set to default values as produced by Autodock 4 utility scripts available with the AutoDockTools package.

**Preparation of Proteins and Ligands for Docking.** Preparation of ligand and receptor were performed using Autodock 4 utility scripts supplied with the software. To prepare the receptors, we ensured that atoms were assigned the correct AutoDock 4 atom types, added Gasteiger charges, merged nonpolar hydrogens, and detected aromatic carbons if present. Preparing the ligand involved the same procedure in addition to setting up a 'torsion tree' defining which bonds

are rotatable. As we have filtered the drug database to only those molecules with less than 10 rotatable bonds, no restriction of the full torsion tree was necessary.

**Docking Results and Normalization.** For each docking, we recorded as the Docking Score the lowest binding energy of the biggest cluster and the corresponding conformer coordinates in a PDB file. Previously, it has been shown that normalizing across targets helps in correctly identifying ligand/receptor pairs.<sup>13</sup> As all the FDA drugs do not have the same size, the same charge, etc., and all the receptors do not present the same binding pocket shape, these factors can increase or decrease docking scores across all targets or across all ligands. For example, a small molecule will generally be able to dock better across a range of binding pocket conformations, and a deeper binding pocket may lead to larger binding affinity, simply because more interactions with the ligand can be established. We could also speculate that a particular choice of settings and parameters for the docking algorithm may favor some targets/ligands over others in a nonspecific way. We can see these biases in the raw scores table (Figure S1). The normalization to correct for these biases can be done in various ways. Normalization can be on a receptor by receptor basis to solve the problem of different sizes of FDA drugs or alternatively on a drug by drug basis to solve the problem of different shapes of receptor binding pockets. Here, we apply both receptor and ligand normalization. The normalization we applied subtracts the mean of column/row raw docking scores from the column/row and then divides by the standard deviation (equivalent to computing a Z-score). When transforming both columns and rows, the procedure was iterated a number of times. The goal is to choose the normalization, which returns the true positives at the top of the ranked normalized list. We defined a Normalized Docking Score for each ligand–target match, based on iterating normalization of targets and then ligands 10 times. The score is strongly negative for ligands that dock well to the target.

**Calculating Interaction Scores with LIGPLOT.** LIGPLOT is a tool which automatically generates schematic diagrams of protein–ligand interactions.<sup>14</sup> The interactions shown are those mediated by hydrogen bonds and by hydrophobic contacts. For each docked ligand, we compared hydrogen bonds and nonbonded contacts to those established by the native structure peptide or small molecule complex. The Interaction Score is then defined as

$$\text{Interaction Score} = a/b$$

where *a* is the number of contact points on the receptor that is shared between the native ligand and the docked ligand, and *b* is the total number of contact points on the receptor for the native ligand alone. According to this formula, a separate interaction score is computed for the H-bond contact points and the nonbonded contact points. The Interaction Score lies between 0 and 1 but is not symmetric like the Tanimoto index, in that switching the identity of docked and native ligand generally yields a different numerical value, but it does not punish a docked ligand for having more interactions than the native peptide, as the Tanimoto index would effectively do. The higher the score, the better the similarity of the interactions between native and docked ligands. The Normalized Interaction Score is then defined as

(Normalized H-bond Interaction Score +  
Normalized Nonbonded Interaction Score)/ $\sqrt{2}$

Note that this implicitly gives equal weight to each type of interaction.

**Combined Docking and Interaction Scores.** As both the docking and interaction scores are separately normalized, they are on the same scale, and we then add the Normalized Docking Score to the negative of the Normalized Interaction Score (favorable docking scores are more negative; favorable interaction scores are more positive; the sign change means that the favorable combined score is more negative). Those with better combined ranking not only show favorable binding to the domains but establish the same interactions with the domain residues, making it a better potential candidate for mimicking the crystal structure peptide ligand or small molecule. It should be noted that this implicitly gives equal weight to the docking scores and the interaction scores, which may not be optimal. In particular, the native ligands for the true positives will always be able to establish the same interactions in the docked and crystal structures which somewhat biases the interaction score to favor true positives. However, by applying the same symmetric normalization to interaction scores as we used for docking scores, we presumably remove some of this bias. As a partial confirmation of this hypothesis, we allowed some flexibility and defined a combined score with a free weighting parameter

$$\text{Combined Score} = w(\text{Normalized Docking Score}) + (1 - w)(-\text{Normalized Interaction Score})$$

and found that optimizing the weight,  $w$ , to maximize the ranking of the true positives gives  $w = 0.4$ , and the change in ranking is marginal if we choose equal weights ( $w = 0.5$ ). For a simpler explanation, we applied equal weights in the final ranking.

## RESULTS AND DISCUSSION

**Importance of Normalization of Docking Scores.** The goal of normalization is to produce a score which preferentially enriches for true positives within the highest ranked compounds: if we see true positive ligand receptor interactions being ranked highly with a normalized score, then we place more confidence in the highly ranked predictions of unknown compound receptor interactions. Thus, we examined the number of true positives within the first 1% of scores. We found that ranking after a symmetric normalization procedure (normalizing scores iteratively by columns and then by rows, repeating this procedure a total of 10 times) yields many true positive interactions and removes receptor and ligand biases apparent in the raw scores (Figure S1, S2). We noted that this iterative normalization procedure does not converge to a fixed set of values, but 10 iterations was sufficient to yield good results for this particular data set size and structure. In addition, the order of transformation, row then column or column then row, generally produces different results, but we chose the latter, as it enriched for more true positive interactions (data not shown).

In Figure 1, we show the percentage of true positives 'discovered' by selecting the top ranked compounds by score. In all, there are 10 570 compound receptor docking scores. The diagonal (bottom line) represents what will happen if compound receptor pairs are chosen randomly: there is no

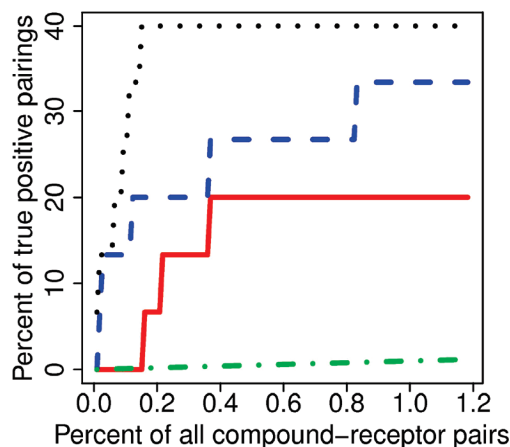


**Figure 1.** Percentage of true positive ligand/receptor pairs in a ranked list of all pairs based on various scores. Docking Scores: solid line; Normalized Docking Scores: dashed line; Combined Score (normalized docking score combined with matching native ligand interactions): dotted line; random expectation: dashed-dotted line.

enrichment for the selection of true positive ligand receptor combinations. All the lines (raw scores and normalized scores) are above the diagonal which is a positive result for using docking to identify compounds that genuinely bind to proteins. We note that Normalized Docking Scores outperform untransformed (raw) Normalized Docking Scores, and that performance is considerably improved using the combined score, utilizing information from both the Normalized Interaction Score and the Normalized Docking Score.

Moreover, using the Combined Score, we observe that 7/15 of the true positive ligands have the lowest normalized score for their native receptor, and 4/15 of the true positive receptors have the lowest normalized score for their native ligand, a criterion which was used in Vigers and Rizzi.<sup>13</sup> In Table 1, we see the top 20 ranked compound-receptor matches. Within the list we recover 6 out of 15 of the true positive interactions which strengthens the belief in the remaining predicted interactions. We further evaluated the evidence for the predicted drug binders by (1) visualization of the docked complex versus the original native crystal complex, by (2) a literature search for information concerning a known interaction with the target, or with a pathway involving the target or an interaction of a related compound/drug with the target.

**HP1 Chromo Shadow Domain.** The Heterochromatin Protein 1 (HP1) or Chromobox Homologue is a nuclear-associated protein with histone binding and DNA silencing functions. It contains a pair of peptide binding domains (chromo shadow domains) forming a dimer. Short peptide recognition occurs by sandwiching the extended peptide between strands of each monomer domain to form an augmented  $\beta$  sheet.<sup>15</sup> The predicted docked compound, **1**, is a HIV-1 protease inhibitor peptidomimetic (Ligand ID: INT<sup>16</sup>) which establishes all five of the same backbone interactions as the peptide motif (see Supporting Information, Figure S3) and also carries hydrophobic side-chain mimetics. HIV-1 protease inhibitors such as **1** and protease inhibitors in general are designed to mimic  $\beta$  strands,<sup>17</sup> the usual conformation of peptides that undergo cleavage, so it is plausible that the predicted interaction would indeed occur. The HP1 protein is important in suppressing breast cancer

**Table 1.** First 20 Compound Domains in Combined Ranked List<sup>a</sup>

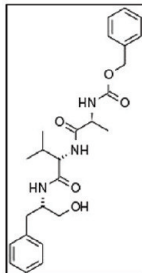
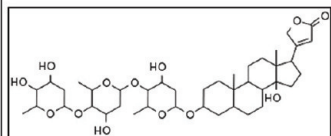
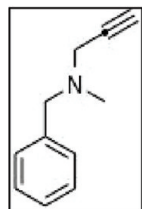
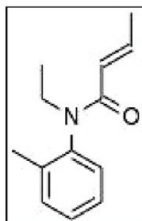
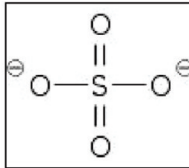
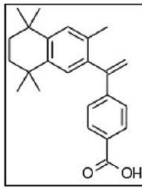
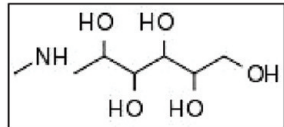
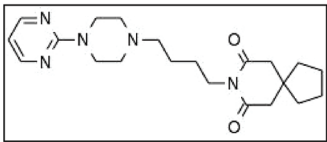
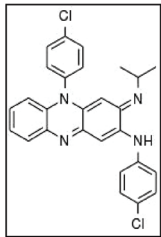
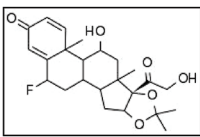
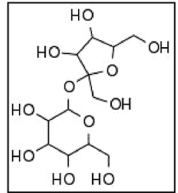
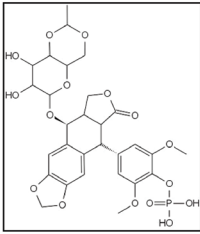
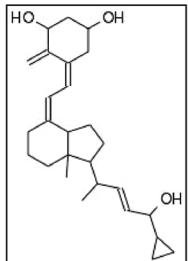
LIGAND	RECEPTOR	AD4 score	Int. score	Final score	Structure	#
ML-IAP/XIAP ligand	ML-IAP/XIAP	-11.28	-1.95	-5.86		
FactorVIIa ligand	FactorVIIa	-11.08	-1.62	-4.45		
INT HIV protease inhibitor	HP1 shadow chromo domain	-9.13	-1.5	-4.33		1
Digitoxin	WW1 domain	-9.04	-0.77	-3.83		2
Pargyline	Bcl-2	-6.05	-0.36	-3.83		3
Crotamiton	Bcl-2	-6.58	-0.34	-3.77		4
Renin ligand	Renin	-9.16	-0.71	-3.72		
Magnesium Sulfate	14-3-3	-5.59	-0.46	-3.58		5
Bexarotene	NR box	-7.96	-0.75	-3.47		6
Bcl-2 ligand	Bcl-2	-10.76	-0.5	-3.37		
Meglumine	Integrin alphaVbeta3	-9.18	-0.87	-3.33		7



Table 1. Continued

LIGAND	RECEPTOR	AD4 score	Int. score	Final score	Structure	#
Thrombin ligand	Thrombin	-8.65	-1.39	-3.27		
Integrin alphaVbeta3 ligand	HIV-1 protease (1dif)	-10.29	-0.53	-3.24		
Buspirone	Cyclin A	-9.02	-1.02	-3.24		8
Clofazimine	MDM2	-8.35	-0.82	-3.23		9
MDM2 ligand	MDM2	-8.09	-0.91	-3.23		
Flunisolide	Dynein DLC8	-7.66	-0.68	-3.17		10
Sucrose	ML-IAP/XIAP	-8.34	-1.19	-3.16		11
Etoposide phosphate	WW1 domain	-7.24	-0.87	-3.15		12
Calcipotriol	HIV-1 protease (1yt9)	-9.1	-1.26	-3.14		13

<sup>a</sup> The yellow rows are true positive matches. The ligand column contains the drug name or three-letter ligand code from MSDchem. The domain/protein name is in parentheses if the structure came from different PDB entries. AD4 score is untransformed AutoDock4 estimated free energy score. Int. Score is the negative of the sum of the Tanimoto scores for H-bond and nonbonded contact similarity: total similarity would give a score of -2. The final score is the sum of the symmetrically normalized AD4 and interaction scores, which we use to rank predicted ligand receptor binding. Structures and compound numbers are given for those discussed further in the text.

metastasis,<sup>18</sup> and modulation of pathways involving it may be of interest in the future.

**WW1 Domain.** The WW1 domain, so-called because of two conserved tryptophan residues, is a small  $\beta$  sheet structure

that preferentially binds proline rich peptides and can often share recognition of peptide sequences with the SH3 domain.<sup>19</sup> The structure for the WW domain (PDB ID: 1eg4<sup>20</sup>) comes from human dystrophin, an essential musculoskeletal protein, of

which impaired function causes muscular dystrophy. We find a cardiac glycoside, **2** (digitoxin), as having very strong affinity for the domain. Digitoxin is used in the treatment of cardiac arrhythmias, where its apparent mechanism of action is to modulate the activity of the sodium ATPase transporter pump.<sup>21</sup> Digitoxin, being a glycoside, contains many oxygen groups capable of establishing hydrogen bonds. Even though the canonical WW1 domain peptide binding motif PP.Y is not very obviously charged or polar with respect to side-chain composition, the full sequence bound in the structure has a backbone H-bond donor interaction with a WW hydroxyl group and two C=O acceptor groups from the peptide backbone. The glycoside establishes H-bond interactions with polar Tyr and Thr residues in the binding site. We note that some evidence exists in the literature that dystrophic subjects show increased sensitivity to the closely related molecule digoxin,<sup>22</sup> and that digitoxin can in fact lead to accelerated muscle wasting,<sup>23</sup> consistent with an already compromised dystrophin protein being further inhibited in forming complexes. Interestingly, digitoxin was demonstrated to have antiproliferative effects on tumor cell lines.<sup>24</sup> Our second match against the WW domain, compound **12** (etoposide phosphate), is an antineoplastic agent which is thought to interfere with DNA topoisomerase and may have a secondary action in interfering with the JNK stress response pathway.<sup>25</sup> Thus, it is potentially possible for both these compounds to have actions via WW signaling. If this is the case, which WW domains are the most likely mediators of such effects? Transiently activated JNK kinase interacts with a WW domain containing pro-apoptotic protein, WOX1, and appears to block its apoptotic function.<sup>26</sup> Second, the antiproliferative effect of digitoxin has been hypothesized to relate to inhibition of the WOX1-interactor, of TNF receptor death-associated domain (TRADD), and of TNF receptor complex formation.<sup>27</sup> These clues suggest the WOX1 WW domain as a target worthy of investigation, although other less studied WW domain-containing proteins may also be good candidates.

**Bcl-2.** Bcl-2 (B-cell leukemia 2) suppresses apoptosis in a variety of cells. It regulates cell death by controlling mitochondrial membrane permeability and appears to directly impair caspase activation.<sup>28</sup> Bcl-2 is just one of a family of Bcl-2 proteins, all of which contain at least one BH3 peptide binding domain. The family members divide into those that are pro- or antiapoptotic. Bcl-2 can form a complex with the pro-apoptotic members Bax or Bak, thereby sequestering them, through an interaction mediated by short peptide sequences. The predicted BH3 binders are **3** (pargyline), a monoamine oxidase inhibitor with antihypertensive properties, and **4** (crotamiton), a scabical and antipruritic agent available as a cream or lotion for topical use only. Both compounds have very similar structure: small, relatively nonpolar, and possessing a phenyl moiety. We find that the docked position of each compound superimposes very closely on the terminal phenyl ring of a known inhibitor (PDB ID: 1ysw, LIGAND code: 43B<sup>29</sup>) against which the FDA drugs were searched. They appear to be involved in a stacking interaction with Phe 109 and Phe 150 of the Bcl-2 protein (Figure 2 and Figure S5). The high affinity inhibitor 43B was built up from fragments using a high throughput NMR screening method,<sup>30</sup> and within the fragments we see structures which resemble the pargyline and crotamiton drugs

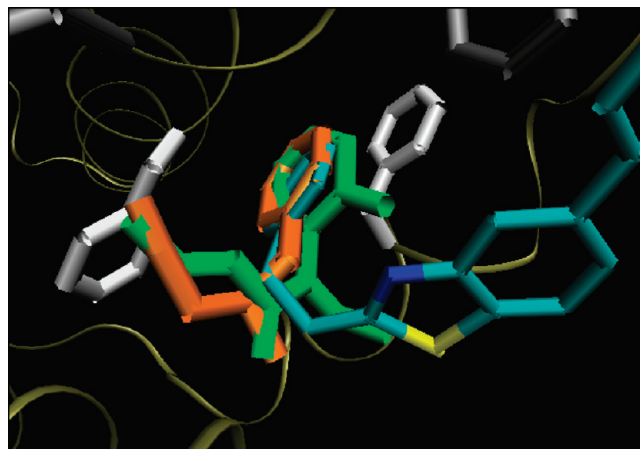


**Figure 2.** Overlap of peptide 43B (light blue) and docked drugs, crotamiton (green) and pargyline (orange). Bcl-2 (gold ribbon). Phe 109 and 150 residues of Bcl-2 are white, and other Phe residues of Bcl-2 are gray.

(e.g., in PDB ID: 1ysg), binding with an estimated dissociation constant approximately = 0.3 mM. Furthermore, we find a crotamiton-related compound (CID 1555866, Tanimoto index 0.61) in a screen for Bcl-B inhibitors, another Bcl-2 family antiapoptotic member (PubChem Bioassay AID: 1243).

**14-3-3 Domain.** The 14-3-3 domain is a domain involved in many cell signaling networks and is known to have multiple interaction partners. It recognizes a phosphorylated serine or threonine motif, with canonical recognition sequence R[SFYW].S.P according to the ELM database.<sup>7</sup> We find a number of potential binders to 14-3-3 domains, which all have in common negative charge and polarity due to the presence of phosphate, sulfate, or carboxyl groups. Indeed, all the docked compounds preferentially locate at the phosphate group position of the native peptide which is surrounded by three positively charged residues in the 14-3-3 domain (Lys 49, Arg 56, and Arg 127; see Figure 3a). Many of the observed H-bond interactions in the crystal structure appear localized on the phosphate moiety and in its vicinity. Therefore, it is reasonable to assume that the small negatively charged compounds we predict as binders will have some affinity for the site. As a partial confirmation of this result, we note that citric acid (ranked 56th out of 10570 with a final score of −2.81) does in fact localize to the phosphate site within a solved crystal structure (PDB ID: 1o9c compared with 1o9d), Figure 2b.

**NR Box.** The nuclear receptor (NR) box is a peptide binding site present on the surface of the nuclear receptor family of transcription factor proteins, which include estrogen, androgen, vitamin D, retinoic acid, PPAR, and glucocorticoid receptors. Nuclear receptors also possess a ligand binding site for endogenous hydrophobic agonist ligands (e.g., estradiol, testosterone, vitamin D) and a corepressor binding site which overlaps with the coactivator site. Coactivator binding leads to increased transcription, and corepressor binding reduces transcription.<sup>31</sup> Antagonist ligands are also found that bind the ligand binding site, and they cause a conformational shift that effectively blocks the coactivator site.<sup>32</sup> The query structure we use for the NR box (with a hydrophobic  $\alpha$  helical recognition motif LXXLL bound) is from the glucocorticoid receptor, and against this we find **6** (bexarotene) as a potential binder.

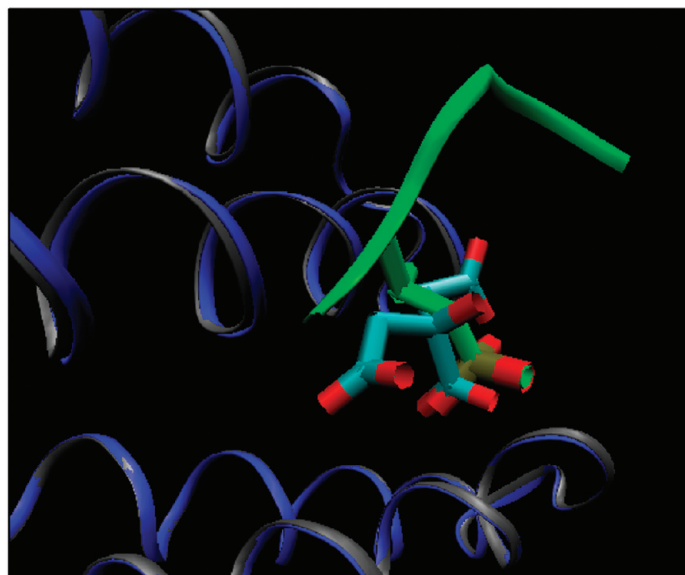
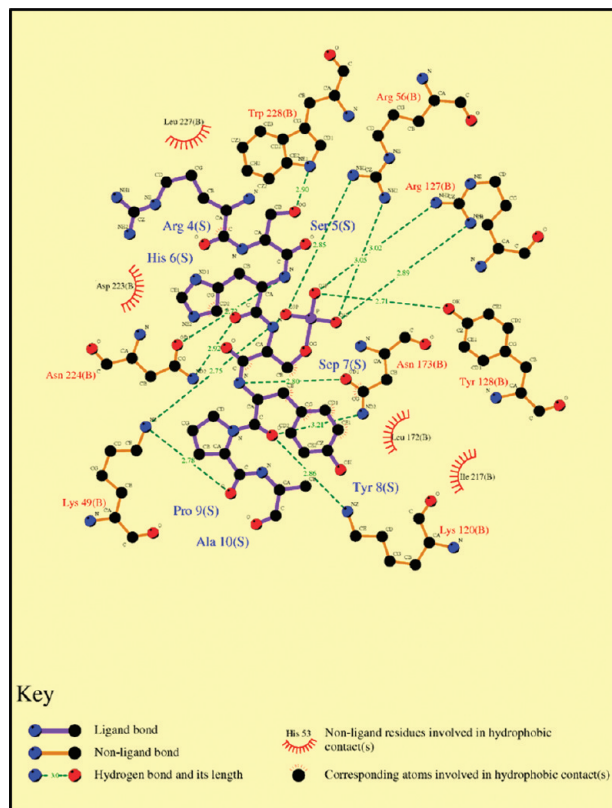


**Figure 3.** (a) LIGPLOT 14-3-3 peptide and domain, and (b) 14-3-3 peptide phosphate and citric acid superposition (from PDB 1o9c and 1o9d). See also Supporting Information, Figure S4.

Bexarotene is an antineoplastic drug that selectively binds and activates the retinoid X (RXR) subfamily of nuclear receptors. The RXR receptors can dimerize with other NR receptors such as vitamin D, retinoic acid receptors (RAR), and PPAR. That a nuclear receptor agonist could also have affinity for the coactivator site, i.e., the NR box, as predicted here has recently been demonstrated experimentally for estrogen receptors, ER  $\alpha$ , ER  $\beta$ ,<sup>33,34</sup> for vitamin D receptors,<sup>35</sup> and computationally for the PPAR coactivator site.<sup>6</sup> We suggest that a similar mechanism may be possible here, although previous studies suggest that bexarotene is selective only for the RXR receptor family. Bexarotene has recently been successfully tested as a topical gel in the treatment of eczema, normally treated with corticosteroids, implying a possible bexarotene glucocorticoid receptor interaction, but more likely due to crosstalk from receptor heterodimerization rather than at the ligand level.<sup>36</sup>

**Integrin  $\alpha_v\beta_3$ .** The RGD tripeptide motif binds integrins in a binding groove at the interface of the heterodimer made up of  $\alpha_v$  and  $\beta_3$  subunits. The RGD motif is present in fibrinogen, an extracellular protein whose attachment to integrin receptors of platelets causes clotting. We see **7** (meglumine), a contrast agent, highly ranked as a potential binder of integrins. Contrast agents such as diatrizoate meglumine and ioxaglate can inhibit the formation of clots in partial thromboplastin time (PTT) assays<sup>37</sup> but are not recorded to have any impact on platelet function. For this reason, we consider it unlikely that meglumine will bind integrins *in vivo*, even though it appears to be able to adopt a conformation that mimics many of the hydrogen bonds of the bound crystal peptide RGD sequence, including the important coordination to the manganese cofactor; see Supporting Information Figure S7.

**Cyclin A.** The cyclin A/CDK2 kinase complex is involved in cell cycle control. A critical interaction occurs with the substrates p21 or p27 which are inhibitors of the cyclin/CDK kinase activity and block cell cycle progression at G1 and thus block cell proliferation. Recognition of cyclin/CDK substrates occurs with the motif [RK].L.{0,1}[FYLVIMP] binding to a groove in cyclin and a phospho-acceptor site [ST]P.[KR] recognized by CDK2. Many inhibitors have been developed to block the recognition site of CDK2, and crystal structures are available for CDK/inhibitor complexes, but inhibitors of the cyclin peptide binding domain are not as common (however, see ligand IDs: C35 and GVC). Peptides based on the p21 or p27 interacting fragments (RXL peptide mimetics) are effective at blocking tumor growth and inducing apoptosis.<sup>38</sup> **8** (buspirone) is an antianxiety agent with high affinity for serotonin receptors and moderate affinity for D2-dopamine receptors.<sup>39</sup> It aligns with the binding groove and effectively mimics the aromatic group of the peptide motif and hydrophobic leucine contacts, and it establishes a backbone H-bond with Ile 281 (Figure S6), though it shares little similarity to the known cyclin A binders, C35 and GVC.

**MDM2.** MDM2 is a ubiquitin ligase anticancer target, as it is a negative regulator of the tumor suppressor transcription factor, p53. The p53/MDM2 interaction is the focus of many computational and experimental screens for small molecule inhibitors.<sup>40</sup> **9** (clofazimine) is a lipophilic dye used as a treatment of mycobacterial infections, due to a supposed mycobacterial DNA binding function.<sup>41</sup> It also appears to have an anti-inflammatory effect against some of the symptoms of mycobacterial infection. Clofazimine shows antitumor activity (bioassay AID: 371<sup>42,43</sup>) and interferes with the NFAT transcription factor pathway (bioassay AID:



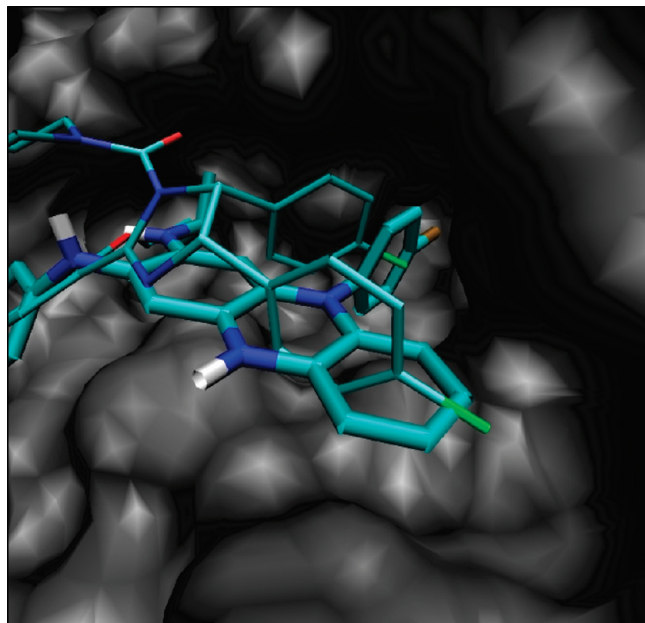


**Figure 4.** MDM2 binding groove (PDB ID: 1rv1) with inhibitor (ligand ID: IMZ, thin sticks) bound and the docked structure, **9**, clofazimine (thick sticks). The chlorine atom (brown) and the phenazine rings on the drug locate to the bromine atoms (green) on IMZ and fill the same large surface cavities.

444) which is directly affected by activated MDM2, although the proposed mechanism for its antiproliferative effects is not mediated by this interaction.<sup>44</sup> It is similar in size to the known inhibitors of p53/MDM2 association, and it appears to bind in the high affinity hydrophobic Trp binding pocket identified in MDM2. The addition of halogen atoms on the Trp residue and on aromatic groups of other MDM2 inhibitors is known to increase binding affinity<sup>1</sup> because of increased shape complementarity within the binding pocket. Clofazimine contains two chlorinated phenyl rings and a branched valine-like terminal group which appear to fill two deep binding cavities on the surface analogous to the bound inhibitor, ligand ID: IMZ, Figure 4.

**Dynein DLC8.** Dynein is an ATP-dependent motor protein that is responsible for protein transport along microtubules and maintains Golgi structure.<sup>45</sup> **10** (flunisolide) is a synthetic corticosteroid and a glucocorticoid receptor agonist. The dynein light chain (DLC) peptide binding motif is [KR].TQT,<sup>7</sup> and its mode of binding is a  $\beta$  augmentation of the DLC8  $\beta$  sheet, exhibiting many backbone and side-chain oxygen and carboxyl interactions in complex. Flunisolide is capable of mimicking these interactions but only captures backbone interactions of the lysine and first threonine residue of the motif. It has recently been noticed that the dynein light chain 8 can inhibit NF- $\kappa$ B transcription, an immune and inflammatory response pathway, through an interaction with the I- $\kappa$ B  $\alpha$  subunit.<sup>46,47</sup> Inhibition of the same pathway occurs with administration of glucocorticoids, including flunisolide, although this is normally considered to occur in a more direct manner by heterodimerization of glucocorticoid receptor and NF- $\kappa$ B.<sup>48</sup>

**ML-IAP/X-IAP.** Melanoma inhibitor of apoptosis (ML-IAP) and X-linked inhibitor of apoptosis (X-IAP) are related antiapoptotic proteins which share a BIR-3 peptide binding domain and are capable of binding caspases thereby blocking their pro-death activities. Overexpression of these proteins

in tumor cell lines has been connected to chemotherapeutic insensitivity, and conversely inhibitors of the BIR-3 domain interactions (such as by the Smac protein) cause resensitization of the tumor cells to cytotoxic factors.<sup>49</sup> An inhibitor of IAP can be as small as a tetrapeptide with consensus motif A[ITV]P[FWIVY] which has two distinct binding pockets: a small N terminal pocket which is predominantly negatively charged and a C-terminal pocket that can incorporate a hydrophobic residue.<sup>49</sup> The N-terminal alanine also establishes backbone interactions in the first pocket. We found a single sucrose molecule, compound **11**, is able to occupy the first (N-terminal pocket) and mimic the peptide interactions, and it forms interactions with Trp 147 protruding from the surface of IAP but is unable to reach to the second binding pocket. It has partial similarity with an antibiotic (Pubchem CID 6473883, Tanimoto coefficient 0.43) which is active as an IAP antagonist (Pubchem Bioassay AID 1018).

## CONCLUSION AND PERSPECTIVES

Protein-protein interactions regulate many biological functions. Discovering new interactions between FDA-approved small molecules and proteins involved in important biological processes such as apoptosis or cell growth signaling would have great therapeutic significance, as the clinical safety and pharmacokinetic profiles of these compounds is already known. In the present work, we have used a docking algorithm to predict the binding tendencies of 287 FDA-approved small molecules against 35 different pockets of proteins which are of the peptide binding class. We developed a normalization procedure that both maximizes the occurrence of true positive compound receptor pairs and ensures that the docked compounds mimic a substantial fraction of the native peptide/ligand's interaction points. As a byproduct, this tends to remove docked compounds that do not bind at the correct position within the domain.

Examination of the scientific literature with respect to the top 20 predictions of compound receptor pairs, we found a number of results worth further investigation, outside of the unambiguous true positive receptor ligand set.

Bcl-2 is a known antiapoptotic protein which has been implicated in the survival of drug-resistant tumors and whose inhibition directly reduces cancer cell proliferation. A number of inhibitors are currently being developed to prevent the formation of Bcl-2 /BAX complexes<sup>29,30,50,51</sup> as well as siRNA molecule targeting which prevents its expression.<sup>52</sup> Two potential Bcl-2 binding compounds were indicated by the docking analysis. Given their small size relative to other high affinity compounds, they would appear less likely to bind with high affinity. Nevertheless, if they show sufficient specificity in particular settings, they could be investigated as cotherapies with other agents targeting this pathway.

The 14-3-3  $\zeta$  protein which is involved in propagating growth signals and is crucial for the proliferation of tumor cells could potentially be inhibited by small acidic molecules which are predicted to bind strongly to the positively charged binding pocket.

The HP1 protein has a DNA silencing and gene regulation function and forms noncovalent bonds through  $\beta$  sheet augmentation of its shadow chromo domain with interaction partners. We found a very plausible interaction with the extended  $\beta$  strand mimetic of the HIV protease inhibitor,



TL-3. While TL-3 is not an approved drug (it entered our study as one of the true positive compounds from known structures<sup>16</sup>), it could provide an interesting lead compound for the investigation of HP1 and its role in tumor metastasis.<sup>18</sup>

The WW domain is present in ubiquitin ligases, kinases, and cytoskeletal proteins. It binds sequence motifs in polyproline rich peptides. The digitoxin cardiac glycoside is a putative binder of the domain, which may suggest alternative modes of action that are related to its antiproliferative function.<sup>53</sup>

We have shown that a systematic docking procedure followed by the correct transformations and analysis of results can lead to significant enrichment of potential actives in a compound database. The choice of compound and receptor database in this study was motivated by speedy translation to clinical development, and tractability for the development of the search strategy. For a number of the drug interactions with peptide binding domains, suggestive clues from the existing literature regarding drug activity or binding provide an additional rationale for prioritizing such matches for further experimental validation.

We believe that dual normalization across ligands and receptors represents an important step in computational drug searching. As described by Warren and co-workers,<sup>54</sup> docking algorithms tend to display widely varying degrees of true positive enrichment for different target proteins, and the set of target proteins that show good enrichment vary from algorithm to algorithm, presumably because of training set selection which affects both protein and compound models. These biases may be mitigated by the post processing of docking scores suggested in this work and other work such as that by Jacobsson.<sup>55</sup> The two-dimensional arrays of raw scores can also be analyzed to determine how the biases arise, by classifying score profiles in terms of molecular descriptors and protein pocket shape and composition. The score profiles themselves can be used to cluster compounds and receptors into similarity classes that may contain more information than that of traditional QSAR descriptors, as they capture modes of interaction rather than static conformations. Selection for the correct mode of interaction is achieved by adding another term to the scores which rewards configurations that mimic the native peptide/ligand interaction points, and we show how that significantly improves the enrichment for true positives.

A future extension would be to apply the same approach to pharmacophore searching, which allows for greatly increased compound database size and would presumably improve scoring and ranking, as previous work<sup>6</sup> indicates that the pharmacophore search is also biased toward certain molecular features. A selection of top ranked matches from such a pharmacophore search or the most highly scored docked poses in this study could be also regarded as initial configurations for extensive molecular dynamics simulations, which provide extra information about the stability of the interaction and explicit solvent effects and allow for more accurate free energy predictions.<sup>56–58</sup>

The computational cost of the scoring procedure remains relatively small, in comparison with the computational cost of docking. The true cost, therefore, lies in the requirement to dock not only a single target of interest but a series of other targets. Parallelized computer systems, such as the Irish Centre for High-End Computing used in this study, are

making such computational approaches feasible. For a given drug library, once the initial investment is made for a diverse series of targets, additional targets may be added to the results database at little extra computational cost.

**Abbreviations.** Bcl-2, B cell leukemia-2; ELM, eukaryotic linear motif; FDA, Food and Drug Administration; MOE, molecular operating environment; rmsd, root mean square deviation; PDB, protein data bank.

## ACKNOWLEDGMENT

This work was supported by the Irish Research Council for Science, Engineering and Technology (IRCSET), and by Science Foundation Ireland (SFI). We thank the Irish Centre for High-End Computing for the use of computing resources.

**Supporting Information Available:** Additional information as noted in the text. This material is available free of charge via the Internet at <http://pubs.acs.org>.

## REFERENCES AND NOTES

- (1) Vassilev, L. T.; et al. In Vivo Activation of the P53 Pathway by Small-Molecule Antagonists of Mdm2. *Science* **2004**, *303* (5659), 844–848.
- (2) Arkin, M. R.; Wells, J. A. Small-Molecule Inhibitors of Protein-Protein Interactions: Progressing towards the Dream. *Nat. Rev. Drug Discovery* **2004**, *3*, 301–317.
- (3) Reixach, N.; Adamski-Werner, S. L.; Kelly, J. W.; Koziol, J.; Buxbaum, J. N. Cell Based Screening of Inhibitors of Transthyretin Aggregation. *Biochem. Biophys. Res. Commun.* **2006**, *348* (3), 889–897.
- (4) Sun, H. Pharmacophore-Based Virtual Screening. *Curr. Med. Chem.* **2008**, *15* (10), 1018–1024.
- (5) Toba, S.; Srinivasan, J.; Maynard, A. J.; Sutter, J. Using Pharmacophore Models To Gain Insight Into Structural Binding and Virtual Screening: An Application Study with Cdk2 and Human Dhfr. *J. Chem. Inf. Model.* **2006**, *46*, 728–735.
- (6) Parathasarathi, L.; Casey, F.; Stein, A.; Aloy, P.; Shields, D. C. Approved Drug Mimics of Short Peptide Ligands from Protein Interaction Motifs. *J. Chem. Inf. Model.* **2008**, *48*, 1943–1948.
- (7) Puntervoll, P.; et al. Elm Server: A New Resource for Investigating Short Functional Sites in Modular Eukaryotic Proteins. *Nucleic Acids Res.* **2003**, *31* (13), 3625–3630.
- (8) Stein, A.; Aloy, P. Contextual Specificity in Peptide-Mediated Protein Interactions. *PLoS ONE* **2008**, *3* (7), e2524.
- (9) Wishart, D. S.; et al. DrugBank: A Comprehensive Resource for in Silico Drug Discovery and Exploration. *Nucleic Acids Res.* **2006**, *34*, D668–672.
- (10) Chemical Computing Group Inc. Molecular Operating Environment, Version 2008.08. Montreal, Canada.
- (11) Huey, R.; Morris, G. M.; Olson, A. J.; Goodsell, D. S. A Semiempirical Free Energy Force Field with Charge-Based Desolvation. *J. Comput. Chem.* **2007**, *28*, 1145–1152.
- (12) Morris, G. M.; Goodsell, D. S.; Halliday, R. S.; Huey, R.; Hart, W. E.; Belew, R. K.; Olson, A. J. Automated Docking Using a Lamarckian Genetic Algorithm and Empirical Binding Free Energy Function. *J. Comput. Chem.* **1998**, *19*, 1639–1662.
- (13) Vigers, G. P.; Rizzi, J. P. Multiple Active Site Corrections for Docking and Virtual Screening. *J. Med. Chem.* **2004**, *47*, 80–89.
- (14) Wallace, A. C.; Laskowski, R. A.; Thornton, J. M. Ligplot: A Program To Generate Schematic Diagrams of Protein-Ligand Interactions. *Protein Eng.* **1995**, *8*, 127–134.
- (15) Brasher, S. V.; Smith, B. O.; Fogh, R. H.; Nietlispach, D.; Thiru, A.; Nielsen, P. R.; Broadhurst, R. W.; Ball, L. J.; Murzina, N. V.; Laue, E. D. The Structure of Mouse Hsp1 Suggests a Unique Mode of Single Peptide Recognition by the Shadow Chromo Domain Dimer. *EMBO J.* **2000**, *19* (7), 1587–1597.
- (16) Li, M.; Morris, G. M.; Lee, T.; Laco, G. S.; Wong, C. H.; Olson, A. J.; Elder, J. H.; Wlodawer, A.; Gustchina, A. Structural Studies of FIV and HIV-1 Proteases Complexed with an Efficient Inhibitor of FIV Protease. *Proteins* **2000**, *38*, 29–40.
- (17) Loughlin, W. A.; Tyndall, J. D. A.; Glenn, M. P.; Fairlie, D. P. Beta-Strand Mimetics. *Chem. Rev.* **2004**, *104*, 6085–6117.
- (18) Norwood, L. E.; et al. A Requirement for Dimerization of Hsp1 in Suppression of Breast Cancer Invasion. *J. Biol. Chem.* **2006**, *281*, 18668–18676.

- (19) Wintjens, R.; Wieruszkeski, J. M.; Drobecq, H.; Rousselot-Pailley, P.; Buée, L.; Lippens, G.; Landrieu, I. <sup>1</sup>H NMR Study on the Binding of Pin1 Trp-Trp Domain with Phosphothreonine Peptides. *J. Biol. Chem.* **2001**, 276 (27), 25150–25156.
- (20) Huang, X.; Poy, F.; Zhang, R.; Joachimiak, A.; Sudol, M.; Eck, M. J. Structure of a WW Domain Containing Fragment of Dystrophin in Complex with Beta-Dystroglycan. *Nat. Struct. Biol.* **2000**, 7, 634–638.
- (21) Bluschke, V.; Bonn, R.; Greeff, K. Increase in the (Na<sup>+</sup> + K<sup>+</sup>)-ATPase Activity in Heart Muscle after Chronic Treatment with Digitoxin or Potassium Deficient Diet. *Eur. J. Pharmacol.* **1976**, 37 (1), 189–191.
- (22) Saito, K.; Ohkura, H.; Kashima, T.; Tanaka, H. Enhanced Sensitivity to Digoxin in Dystrophic Mice. *Jpn. Heart J.* **1984**, 25, 765–777.
- (23) Heyck, H.; Laudahn, G.; Luders, C. J.; Muller-Stephann, H.; Schmidt-Peter, P. Anabolic Steroids and Digitoxin in the Treatment of Progressive Muscular Dystrophy. *Acta Paediatrica* **1965**, 54 (3), 205–221.
- (24) Lopez-Lazaro, M.; Pastor, N.; Azrak, S. S.; Ayuso, M. J.; Austin, C. A.; Cortes, F. Digitoxin Inhibits the Growth of Cancer Cell Lines at Concentrations Commonly Found in Cardiac Patients. *J. Nat. Prod.* **2005**, 68 (11), 1642–1645.
- (25) Anderson, S. M.; et al. Etoposide-Induced Activation of C-Jun N-Terminal Kinase (Jnk) Correlates with Drug-Induced Apoptosis in Salivary Gland Acinar Cells. *Cell Death Differentiation* **1999**, 6 (5), 454–462.
- (26) Chang, N.-S.; et al. Molecular Mechanisms Underlying Wox1 Activation during Apoptotic and Stress Responses. *Biochem. Pharmacol.* **2003**, 66 (8), 1347–1354.
- (27) Yang, Q.; et al. Cardiac Glycosides Inhibit TNF- $\alpha$ /NF- $\kappa$ B Signaling by Blocking Recruitment of Tnf Receptor-Associated Death Domain to the Tnf Receptor. *Proc. Natl. Acad. Sci. U.S.A.* **2005**, 102 (27), 9631–9636.
- (28) Allen, R. T.; Cluck, M. W.; Agrawal, D. K. Mechanisms Controlling Cellular Suicide: Role of Bcl-2 and Caspases. *Cell. Mol. Life Sci.* **1998**, 54, 427–445.
- (29) Oltersdorf, T.; et al. An Inhibitor of Bcl-2 Family Proteins Induces Regression of Solid Tumours. *Nature* **2005**, 435, 677–681.
- (30) Shuker, S. B.; Hajduk, P. J.; Meadows, R. P.; Fesik, S. W. Discovering High-Affinity Ligands for Proteins: Sar by NMR. *Science* **1996**, 274, 1531–1533.
- (31) Horwitz, K. B.; Jackson, T. A.; Bain, D. L.; Richer, J. K.; Takimoto, G. S.; Tung, L. Nuclear Receptor Coactivators and Corepressors. *Mol. Endocrinol.* **1996**, 10, 1167–1177.
- (32) Hashimoto, Y.; Miyachi, H. Nuclear Receptor Antagonists Designed Based on the Helix-Folding Inhibition Hypothesis. *Bioorg. Med. Chem.* **2005**, 13 (17), 5080–5093.
- (33) Jensen, E. V.; Khan, S. A. A Two-Site Model For Antiestrogen Action. *Mechanisms of Ageing and Development* **2004**, 125 (10), 679–682.
- (34) Wang, Y.; Chirgadze, N. Y.; Briggs, S. L.; Khan, S.; Jensen, E. V.; Burris, T. P. A Second Binding Site for Hydroxytamoxifen within the Coactivator-Binding Groove of Estrogen Receptor Beta. *Proc. Natl. Acad. Sci. U.S.A.* **2005**, 103 (26), 9908–9911.
- (35) Mizwicki, M. T.; et al. Identification of An Alternative Ligand-Binding Pocket in the Nuclear Vitamin D Receptor and Its Functional Importance in 1 $\alpha$ ,25(OH)<sub>2</sub>-Vitamin D<sub>3</sub> Signaling. *Proc. Natl. Acad. Sci. U.S.A.* **2004**, 101, 12876–12881.
- (36) Kuenzli, S.; Tran, C.; Saurat, J. H. Retinoid Receptors in Inflammatory Responses: A Potential Target for Pharmacology. *Current Drug Targets: Inflammation and Allergy* **2004**, 3 (4), 355–360.
- (37) Farrehi, P. M.; Zhu, Y.; Fay, W. P. An Analysis of Mechanisms Underlying the Antifibrinolytic Properties of Radiographic Contrast Agents. *J. Thrombosis and Thrombolysis* **2001**, 12 (3), 273–281.
- (38) Mendoza, N.; Fong, S.; Marsters, J.; Koeppen, H.; Schwall, R.; Wickramasinghe, D. Selective Cyclin-Dependent Kinase2/Cyclin A Antagonists That Differ from Atp Site Inhibitors Block Tumor Growth. *Cancer Res.* **2003**, 63, 1020–1024.
- (39) de Boer, S. F.; Lesourd, M.; Mocaer, E.; Koolhaas, J. M. Selective Antiaggressive Effects of Alnespiron in Resident-Intruder Test Are Mediated via 5-Hydroxytryptamine1A Receptors: A Comparative Pharmacological Study with 8-Hydroxy-2-dipropylaminotetralin, Ipsapirone, Buspirone, Eltoprazine, and Way-100635. *J. Pharmacol. Exp. Ther.* **1999**, 288 (3), 1125–1133.
- (40) Buolamwini, J. K.; Addo, J.; Kamath, S.; Patil, S.; Mason, D.; Ores, M. Small Molecule Antagonists of the Mdm2 Oncoprotein as Anticancer Agents. *Curr. Cancer Drug Targets* **2005**, 5, 57–68.
- (41) Morrison, N. E.; Marley, G. M. Clofazimine Binding Studies with Deoxyribonucleic Acid. *Int. J. Lepr Other Mycobact Dis* **1976**, 44 (4), 475–481.
- (42) Pourgholami, M. H.; Lu, Y.; Wang, L.; Stephens, R. W.; Morris, D. L. Regression of Novikoff Rat Hepatocellular Carcinoma Following Locoregional Administration of a Novel Formulation of Clofazimine in Lipiodol. *Cancer Lett.* **2004**, 207 (1), 37–47.
- (43) Van Rensburg, C. E.; Joone, G. K.; O'Sullivan, J. F. Clofazimine and B4121 Sensitize an Intrinsically Resistant Human Colon Cancer Cell Line to P-Glycoprotein Substrates. *Oncol. Rep.* **2000**, 7 (1), 193–195.
- (44) Van Rensburg, C. E. J.; Van Staden, A. M.; Anderson, R. The Riminophenazine Agents Clofazimine and B669 Inhibit the Proliferation of Cancer Cell Lines in Vitro by Phospholipase A2-Mediated Oxidative and Nonoxidative Mechanisms. *Cancer Res.* **1993**, 53, 318–323.
- (45) Corthesy-Theulaz, I.; Pauloin, A.; Pfeffer, S. R. Cytoplasmic Dynein Participates in the Centrosomal Localization of the Golgi Complex. *J. Cell Biol.* **1992**, 118 (6), 1333–1345.
- (46) Jung, Y.; Kim, H.; Min, S. H.; Rhee, S. G.; Jeong, W. Dynein Light Chain Lc8 Negatively Regulates NF- $\kappa$ B through the Redox-Dependent Interaction with I $\kappa$ B $\alpha$ . *J. Biol. Chem.* **2008**, 283 (35), 23863–23871.
- (47) Crepieux, P.; et al. I $\kappa$ B $\alpha$  Physically Interacts with a Cytoskeleton-Associated Protein through Its Signal Response Domain. *Mol. Cell. Biol.* **1997**, 17 (12), 7375–7385.
- (48) Widen, C.; Gustafsson, J. A.; Wikstrom, A. C. Cytosolic Glucocorticoid Receptor Interaction with Nuclear Factor-Kappa B Proteins in Rat Liver Cells. *Biochem. J.* **2003**, 372, 211–220.
- (49) Zobel, K.; et al. Design, Synthesis, and Biological Activity of a Potent Smac Mimetic That Sensitizes Cancer Cells to Apoptosis by Antagonizing Iap. *ACS Chem. Biol.* **2006**, 1 (8), 525–533.
- (50) Enyedy, I. J.; et al. Discovery of Small-Molecule Inhibitors of Bcl-2 Through Structure-Based Computer Screening. *J. Med. Chem.* **2001**, 44, 4313–4324.
- (51) Tzung, S.-P.; et al. Antimycin A Mimics a Cell-Death-Inducing Bcl-2 Homology Domain 3. *Nat. Cell Biol.* **2001**, 3, 183–191.
- (52) Anderson, E. M.; et al. Gene Profiling Study of G3139- and Bcl-2-Targeting Sirnas Identifies a Unique G3139 Molecular Signature. *Cancer Gene Ther.* **2006**, 13, 406–414.
- (53) Winnicka, K.; Bielawski, K.; Bielawska, A. Cardiac Glycosides in Cancer Research and Cancer Therapy. *Acta Pol. Pharm.* **2006**, 63 (2), 109–115.
- (54) Warren, G. L.; et al. A Critical Assessment of Docking Programs and Scoring Functions. *J. Med. Chem.* **2006**, 49, 5912–5931.
- (55) Jacobsson, M.; Karlen, A. Ligand Bias of Scoring Functions in Structure-Based Virtual Screening. *J. Chem. Inf. Model.* **2006**, 46 (3), 1334–1343.
- (56) Alonso, H.; Bliznyuk, A. A.; Gready, J. E. Combined Docking and Molecular Dynamic Simulations in Drug Design. *Med. Res. Rev.* **2006**, 26 (5), 531–568.
- (57) Moitessier, N.; Henry, C.; Maigret, B.; Chalepur, Y. Combining Pharmacophore Search, Automated Docking, and Molecular Dynamics Simulation as a Novel Strategy for Flexible Docking. Proof of Concept: Docking of Arginine-Glycine-Aspartic Acid-like Compounds into the  $\alpha\sqrt{3}$  Binding Site. *J. Med. Chem.* **2004**, 47, 4178–4187.
- (58) Rapp, C. S.; Schonbrun, C.; Jacobson, M. P.; Kalyanaraman, C.; Huang, N. Automated site preparation in physics-based rescoring of receptor ligand complexes. *Proteins* **2009**, 77, 52–61.

CI900294X